Carbon nanofibers-based nanoconfined liquid phase filtration for the rapid removal of chlorinated pesticides from ginseng extracts

Huaze Sun[1], Yilin Zou[1], Han Yeong Kaw[2], Liyuan Wang[1], Gang Wang[1], John L. Zhou[3], Long-Yue Meng[4], Donghao Li[1, 5, *]

*Corresponding author

1. Department of Chemistry, Yanbian University, Park Road 977, Yanji city, Jilin Province, 133002, PR China.

2. Department of Environmental Science, Zhejiang University, Hangzhou 310058, China.

3. Centre for Green Technology, School of Civil and Environmental Engineering, University of Technology Sydney, 15 Broadway, Australia.

4. Department of Environmental Science, Yanbian University, Park Road 977, Yanji City, Jilin Province, 133002, PR China.

5. Interdisciplinary of Biological Functional Molecules, College of Integration Science, Yanbian University, Park Road 977, Yanji city, Jilin Province, 133002, PR China

ABSTRACT

A rapid nanoconfined liquid phase filtration system (NLPF) based on solvent-confined carbon nanofibers/carbon fibers materials (CNFs/CFs) was proposed to effectively remove chlorinated pesticides from ginsenosides-containing ginseng extracts. A series of major parameters that may affect the separation performance of CNFs-NLPF method were extensively investigated, including the water solubility of nanoconfined solvents, filtration rate, ethanol content of the ginseng extracts and reusability of the material for repeated adsorption. The developed method showed high removal efficiency of pesticides (85.5 - 97.5%), high retainment rate of ginsenosides (95.4 - 98.9%) and consistent reproducibility (RSD < 11.8%). Furthermore, the feasibility of the CNFs-NLPF technique to be scaled-up for industrial application was systematically explored by analyzing large-volume ginseng extract (1 L), which also verified its excellent modifiable characteristic. This filtration method exhibits promising potential as a practical tool for removing pesticide residues and other organic pollutants in food samples to assure food quality and safeguard human health.

Keywords

Carbon nanofibers; Nanoconfined solvent; filtration; Pesticide residues; Ginsenoside

1. INTRODUCTION

Panax ginseng C. A. Meyer (ginseng) is a kind of perennial herb that contains substantial amount of bioactive ingredients.[1] Ginsenosides are the major pharmacological components that constitute 2-3% of ginseng,[2] in which various pharmacological activities of ginsenosides have been revealed, including anti-inflammatory, anticancer, antidiabetic, and antioxidative effects.[3] Throughout the six-year growth period of ginseng crops, pesticide residues in soil are passively absorbed and accumulate in ginseng, especially the organochlorine pesticides with high persistence property.[4–6] During the extraction of ginsenosides, a fraction of these pesticide residues are simultaneously being extracted,[7] which are difficult to be removed as to minimize ginsenosides losses from ginseng extracts. Numerous studies have reported that a long-term exposure to residual chlorinated pesticides is linked to adverse human health effects, such as immune suppression, hormone disruption, reproductive abnormalities and cancer.[8] Therefore, the targeted elimination of pesticide residues is an inevitable step in ginseng processing.

There have been many attempts to develop effective methods for removing pesticide residues, including moving bed biofilm reactor (MBBR),[9,10] advanced oxidation processes (AOPs),[11,12] and adsorption. Despite the fact that these technologies can achieve industrial elimination of pesticide residues, cost-intensive, time-consuming and complicated operations are the common shortcomings. In the current ginseng industry, size exclusion technology with the utilization of macroporous resin has risen to be a more commonly employed method to remove pesticide residues, which is based on the distinct size difference between pesticides and ginsenosides to achieve effective separation. Nevertheless, sophisticated design that relies heavily on the

physicochemical properties of analytes is often required for this technique to accomplish highly selective adsorption. It is, therefore, difficult to simultaneously remove pesticide residues with considerably different properties by using only single-sized macroporous resins, while composite-sized macroporous resins pose a risk of causing the loss of ginsenosides.[13,14] Thus, an adsorbent with high selectivity and large load capacity is urgent needed.

Organic solvents have proved its unique selective extraction capacity across different polarities, which also exhibits extremely fast mass transfer speed and high load capacity.[15] Conventional liquid-liquid extraction (LLE) is infeasible for industrial application because of the laborious operation and large solvent consumption. At present, holder-assisted micro-liter liquid extraction has been widely demonstrated as a solvent-saving, time-saving, and simple technique. Various kinds of substrate-based solvent support phase extraction methods that employed materials like knitting wool,[16] stainless steel wire[17] and melamine foam[18] have been explored, which can extract trace target compounds via loaded solvent. These studies highlighted the potential of flexible material with porous surface which acts as an adsorbent filler or column packing for confining a minimal amount of solvent, and employ it to accurately separate ginsenosides and pesticides based on the distinguishable polarity difference. However, the structural limitations of some substrate materials may lead to some intricate problems, including solvent shedding under vigorous stirring, residues of the analytes, unmodifiable shape and limited modifiability, which make these materials unsuited to be applied in formulating a filter-type separation device to eliminate pesticide residues from ginseng extract.

In recent years, research on carbon material with outstanding properties has been extensively studied.[19] Among which, carbon nanofibers (CNFs) are one of the hotly

considered materials for its bending and entanglement morphologies.[20] Carbon nanofibers that grow on carbon fibers (CNFs/CFs) were previously synthesized by using chemical vapor deposition method (CVD),[21] which demonstrated a state of bending and entanglement to form numerous three-dimensional nanopores between CNFs. A nanoconfined liquid phase nanoextraction technique (NLPNE) based on CNFs had been systematically studied in our previous work.[22] When a certain amount of solvent was added on the CNFs/CFs surface, it was firmly confined within the nanoporous structure of the material. Different solvents were successfully confined on the CNFs/CFs materials, and such an approach favors the selective adsorption of various target compounds according to the liquid phase extraction principle.

In this study, a simple, rapid and efficient carbon nanofibers-based nanoconfined liquid phase filtration (CNFs-NLPF) technique was established for the effective elimination of pesticides from ginseng extract based on the difference in polarities between ginsenosides and pesticides. The non-polar chlorinated pesticides can be effectively removed, while the polar ginsenosides were successfully retained in ginseng extract after treated by this technique. By stacking the CNFs/CFs into a membrane-like filtration material to remove pesticide residues, different types of confined solvents, filtration rate and desorption parameters were systematically optimized in this study. In view of the addition of ethanol in ginseng industry during ginsenosides extraction, the influence of ethanol content on the removal efficiency of pesticide residues in ginseng extract was evaluated. The reusability of the material was also assessed. A laboratorial scale-up version of the filtration device was subsequently fabricated to examine the feasibility of the proposed filtration technique for potential industrial applications.

2. MATERIALS AND METHODS

2.1 Chemicals and reagents

All HPLC grade organic solvents including acetone (ACE), dichloromethane (DCM), hexane (HEX), acetonitrile (ACN), methanol (MeOH) and ethanol (EtOH) were purchased from Thermo Fisher Scientific (Waltham, MA, USA). Reference standards for alpha-hexachlorocyclohexane (α-HCH), gamma-hexachlorocyclohexane (lindane), delta-hexachlorocyclohexane (δ-HCH), pentachloronitrobenzene (PCNB), heptachlor, aldrin, heptachlor epoxide, procymidone, endosulfan (both isomers A and B), dichlorodiphenyldichloroethylene (DDE), dichlorodiphenyldichloroethane (DDD), dichlorodiphenyltrichloroethane (DDT), dieldrin, endrin and methoxychlor with purities of 99.9% were bought from AccuStandard (New Haven, CT, USA). Triphenyl phosphine (TPP) as internal standard was bought from Chem Service (West Chester, PA, USA). The mixed ginsenosides standard comprising Rb1, Rb2, Rc, Re, Rd, Rg1, Rf, which represents the major constituents of ginseng saponins in ginseng,[23–26] was purchased from National Institute for the Control of Pharmaceutical and Biological Products (Beijing, China). Ultrapure water was obtained using a Milli-Q water purification system (Millipore Corporation, Bedford, MA, USA). Polyether sulfone (PES) membrane with a pore size of 0.22 μm was purchased from Jinteng Co. Ltd. (Tianjin, China). A syringe pump (Model XFP01-B, Suzhou Xunfei Co. Ltd., Suzhou, China) was used for regulating the flow rate of filtration.

2.2 Synthesis of CNFs/CFs

The details of CNFs/CFs synthesis have been reported in previous work.[21] In brief, CFs were subjected to thermal debinding before being Soxhlet extracted to burn up the organic binder. The desized CFs were immersed in a solution of HNO_3/H_2SO_4 for 12 h

and then washed with water to obtain a pH level of 7.[27] The acid-treated CFs were impregnated and dispersed in Ni-doped mesoporous silica precursor solution for 12 h and then the CFs were air-dried.[28] The CFs were placed in the middle of a tube furnace and calcined at 1023 K under 150 cm^3 of flowing N_2; they were then subjected to a reduced flow of 10% H_2/N_2 (150 cm^3) for 30 min to obtain the reductive Ni nanoparticles. Acetylene (30 cm^3) was then introduced into the furnace for 30 min to facilitate the growth of CNFs on the surface of the CFs. The morphologies of CFs and CNFs were characterized by scanning electronic microcopy, SEM (Hitachi Regulus 8100, Japan).

2.3 Sample preparation

Ginseng extracts were prepared according to a previous study.[29] In brief, 30 g ginseng sample was mixed with 1 L of water, and then ultrasonicated for 1 h. The mixture was kept overnight at 4 °C and filtered through a filter paper before being employed for evaluating the repeatability of the CNFs/CFs, validation of the developed method and in scaled-up filtration experiments. Different commercially-available ginseng products intended for TCM prescriptions comprising ginseng, American ginseng (*Panax quinquefolius*) and Notoginseng (*Panax notoginseng*) were purchased from a local Chinese medicine store in Yanji city, Northeast China, for the verification of application prospect of this method. To evaluate the separation performance of the CNFs-NLPF technique, a series of optimization experiments were carried out by using pesticides and ginsenoside standards solutions. A mixed standard solution with four representative pesticides including DDT, PCNB, lindane and procymidone was prepared at 10 mg kg^{-1} by diluting the standard stock solution for each pesticide with acetone. The standard working solutions for spiked standard comprising 0.5 μg g^{-1} chlorinated pesticides and 5 μg g^{-1} ginsenosides were freshly

prepared by diluting the mixed standards solutions with ultrapure water before optimization experiments. A mixed standard solution with all nineteen chlorinated pesticides was prepared at 10 mg kg^{-1} by diluting the standard stock solution for each pesticide with acetone, which was further diluted to prepare the standard working solution at 0.5 μg g^{-1} for assessing the method performance of CNFs/CFs materials in ginseng extract, scale-up experimentations and application in real ginseng products.

A filter-type treatment method was proposed, which is in parallel with the requirements of industrial applications. Approximately 10 (± 0.5) mg of CNFs/CFs were accurately weighed. The weighed CNFs/CFs were evenly filled into the PES membrane, and 50 μL HEX was added onto CNFs/CFs to confine solvent on the material surface. The PES membrane was attached to a syringe, and the filtration system was connected to a syringe pump to evaluate the separation performance.

As for the scale-up version of this filtration technique, the fabrication procedures of this simple device were as follows: the bottom of an open-ended glass cylinder was enclosed with a stopper fitted with a tube for collecting filtered samples, while the other end was similarly enclosed with a stopper with a tube for drawing in sample. The filtration device was connected to a peristaltic pump to control the constant flow rate of filtration. Upon the completion of filtration process, the collected sample in a flask was subsequently used for analyses of pesticide residues and ginsenosides.

The treatment process began with inserting the pre-weighed CNFs/CFs material into the bottom of filtration cylinder. An appropriate volume of HEX was added into the filtration system so that it was fully confined on the material surface. When excessive HEX slowly flowed out from the system, ginseng extract containing tested pesticides was pumped into the column for pesticide removal. When the filtration was completed, an appropriate volume of HEX was added into the system to desorb

organic solvent that contain pesticides from the CNFs/CFs under a constant flow rate. The fully desorbed organic solvent was filtered through a column with anhydrous sodium sulfate to eliminate excessive water content, and the volume of the extract was adjusted to 80 μL. Internal standard was added and 2 μL from the final extract was subjected to GC-MS analysis. The collected ginseng solution containing ginsenosides was detected by LC-MS/MS.

2.4 Instrumental analysis

2.4.1 GC-MS

Pesticide residues were analyzed using a GC2010 gas chromatograph (Shimadzu, Kyoto, Japan) equipped with an Agilent DB-5MS quartz capillary column (30 m × 0.25 mm × 0.25 μm) and coupled to a QP2010 mass spectrometer (Shimadzu, Kyoto, Japan). Helium (purity, 99.999%) was used as the carrier gas at a constant flow rate of 1.0 mL min^{-1}. The injector temperature, ion source temperature and interface temperature of GC-MS were set at 280, 230 and 280°C, respectively. Operating conditions were as follows: the initial temperature 40°C was directly increased to 150°C at 50°C min^{-1} and then increased to 260°C at 5°C min^{-1}. Injections were carried out in splitless mode with an injection volume of 2 μL. Selected ion monitoring (SIM) mode with a sampling rate of 1.0 s was used. The retention times and three characteristics ions including one target and two qualifier ions selected for qualitative and quantitative determination of pesticides are listed in Table 1. Each pesticide compound was confirmed using the retention time match and the intensity ratio of characteristic ions.

2.4.2 LC-MS/MS

For ginsenoside analysis, a HPLC-ESI-MS/MS detection system consisted of an Agilent 1260 HPLC system and an Agilent 6420 triple quadrupole mass spectrometer (Agilent Technologies, Santa Clara, USA) was used. The chromatographic separations

were carried out with a ZORBAX Eclipse XDB-C18 column (4.6 × 150 mm, 5 μm particle size) purchased from Agilent (Wilmington, DE, USA) with a flow rate of 0.5 mL min^{-1}. Solvents used for the HPLC analysis were 0.1% formic acid in H_2O (A) and ACN (B). The column was kept at 25 (± 2) °C and the sample injection volume was 2 μL. Before chromatographic analyses, all the samples were filtered through 0.22 μm polytetrafluoroethylene membranes. A gradient program for the change of mobile phase was as follows: 20 min linear gradient from 63% A and 27% B to 54% A and 46% B; 1 min from 54% A and 46% B to 63% A and 27% B, then the system was re-equilibrated to initial conditions for 5 min. The total run-time was 26 min. The data were acquired in multiple reaction monitoring (MRM) mode, and the precursor ions, product ions, fragment energies and collision energies used for quantification of ginsenosides are indicated in Table 1.

2.5 Evaluation of analytical performance

In order to verify the method performance and to guarantee the quality of the analytical procedure in this study, a standard mixture comprised a total of nineteen chlorinated pesticides were used to evaluate the reproducibility, linearity and method limit of detection (MLOD) of this method. The recovery and precision (RSD%) of this method were investigated by spiking 500 ng g^{-1} in different ginseng samples (n = 3). The concentrations of pesticides ranged from 5 to 1000 ng g^{-1} in spiked ginseng samples were used for linearity evaluation. The MLODs for all pesticides were calculated as three times the signal-to-noise ratio in spiked ginseng samples after CNFs-NLPF filtration.

2.6 Data analysis

The plot of data and significant analysis were performed using Microsoft Excel 2019 (Redmond, WA, USA). The extraction efficiency of chlorinated pesticides

influenced by type of confined solvent, filtration rate, desorption rate and desorption solvent volume were assessed using one-way analysis of variance (ANOVA) with post-hoc comparisons using Tukey HSD test. All the statistically significant differences between groups have been indicated using asterisks in the figures.

3. RESULTS AND DISCUSSION

3.1 CNFs/CFs characterization

The characterization results were shown in Figure 1 (a) and (b), which contain desized CF and modified CNFs/CF, respectively. It can be seen from Figure 1 (b) that the dense, uniform and curvy CNFs grew on the CF surface, resulting in an approximate five-fold increase in diameter. The subfigure in Figure 1 (b) showed that the diameter of the voids formed by grown CNFs ranged between 200 to 500 nm, which provided suitable pore sizes on the material surface for solvent confinement. The difference in specific surface area between CFs and CNFs was previously proven to be thirty-fold increment for CNFs than CFs. The significant increase in specific surface area denoted a large number of porous structures were exposed on the surface of the material. A rich profusion of pores can immobilize a considerable volume of confined solvent, which is beneficial to improve the adsorption performance of the material. Additionally, the confined solvent existed in the form of vastly dispersed nano-droplets on the material surface greatly increases the contact area between two liquid phases, hence expediting the rate of mass transfer.

3.2 Optimization on the influential factors of CNFs-NLPF

The conventional LLE system mainly relies on the distribution equilibrium of the target between aqueous phase and organic phase, which eventually facilitates the

transfer of analytes from aqueous solution into organic solvent to achieve extraction. During the CNFs-NLPF filtration process, the extraction solvents were dispersed into countless nano-droplets on the surface of the material, which greatly increases the contact area between both liquid phases, thus significantly improves extraction efficiency.[30] The property of the confined solvent is the decisive parameter of this method, which directly affects the selective removal of the targets. The velocity of CNFs-NLPF process determines the highest rate of achieving dynamic equilibrium. The desorption process was also explored as it affects the ease of operation, repeatability and stability of material. These influential factors affecting the removal performance of CNFs-NLPF were systematically optimized. The experiments in this section were carried out in triplicate by spiking the mixed standard of four representative pesticides that cover a wide range of polarities, hence they were selected as the analytes for optimization experiments.

3.2.1 Selection of confined solvent

In the case of CNFs-NLPF technique, confined solvent plays a key role in selectively extracting analytes with specific properties. The selection of confined solvents also follows the principle of extraction solvents in LLE, which is based on the different distribution coefficient of targets between two liquid phases. The maximum extraction of the targets can be achieved when the solubility of the targets in the extraction solvent is much greater than that of the original system. In order to realize an effective removal of pesticide residues without losing the content of ginsenosides, the distinguishable properties between these two groups of compounds were firstly examined. Ginsenosides belong to the steroid group with lots of hydrophilic hydroxyl group, hence making them strongly polar compounds that can exist stably in aqueous solutions. In contrast, chlorinated pesticides are a class of lipophilic compounds with

excellent solubility in weakly polar solvents such as DCM and HEX. Therefore, a suitable extraction solvent can achieve the selective adsorption of pesticide residues and effectively allow the retainment of ginsenosides in the ginseng extract. In this study, HEX, DCM and EtOH were sequentially evaluated based on the difference in polarity. To validate the significance of solvent confinement that plays a pivotal role on the extraction performance of this filtration method, the extraction capability of CNFs/CFs material without confining solvents were also assessed. Based on the results in Figure 2(a), it was obvious that the adsorption performance of CNFs/CFs material without solvent confinement was extremely poor if compared to those with organic solvent confined on the material surface. These results justified the importance of solvent confinement on material surface for pesticide adsorption, especially for adsorbing pesticide with comparatively higher polarity like procymidone. By assessing the adsorptive performance between different types of nanoconfined solvents, the removal efficiencies of pesticide residues were over 70.8% in all solvents, but as high as 98.8% ginsenosides were simultaneously eliminated when EtOH was chosen as the confined solvent. It is due to the "like dissolves like" principle in which ginsenosides are inclined to partition to EtOH compared to HEX and DCM. Both HEX and DCM achieved desired results with pesticides removal efficiencies of greater than 85.2% and RSDs of less than 9.3%, while the retention rates of ginsenosides were higher than 92.4% with RSDs of less than 8.0%. HEX was eventually chosen as the most ideal confined solvent as it is commonly used as an extractant for biologically active constituents in medicinal plants or food, hence proving its suitability for CNFs-NLPF method development.[31–34]

3.2.2 Effects of filtration rate

Throughout the dynamic adsorption process for fixed-bed filtration systems, initial concentration and filtration rate are two consequential factors that need to be

considered.[35] In this study, the chosen initial concentration of 500 ng mL^{-1} is much greater than MRLs, which show representativeness that aimed to demonstrate the effectiveness of this filtration technique. The influence of filtration rate, on the other hand, is far more deciding in the CNFs-NLPF system. Under the same initial concentration in the CNFs-NLPF system, the influence of filtration rate on the removal efficiency of pesticides was systematically evaluated. In this section, PCNB was selected as the model analyte to optimize the flow rate for CNFs-NLPF system at 30, 45 and 60 mL min^{-1}, and the adsorption equilibrium curves under different flow rates were demonstrated in Figure 2(b). It can be observed that the breakthrough curve for higher flow rate was comparatively steeper than lower flow rates throughout the filtration. This phenomenon can be explained by the shorter contact time available between pesticide and organic solvent molecules, hence diminishing the efficacy of mass transfer for complete adsorption. Such an explanation has been verified in previous research,[35,36] and it was consistent with the results in this study which recorded a reduction in the rate of pesticide removal from 88.8% to 61.8% when the flow rate was adjusted from 30 to 60 mL min^{-1}, as shown in Figure 2(c). It is important to stress that there were no significant losses of ginsenosides under these three flow rates. After taking the overall effectiveness and efficiency factors into consideration, 45 mL min^{-1} was eventually selected as the optimum flow rate for dynamic adsorption, which achieved removal rate of > 83.3% with the RSDs < 9.5% for all target pesticides in this study.

3.2.3 CNFs-NLPF desorption process

A suitable desorption method is essential for assuring method performance and the reusability of materials. There have been a large number of researches confirming the high degree of flexibility for carbon nanomaterials with non-destructive recovery to its

original state.[37,38] Hypothetically, the solvent-confined CNFs can be symbolized as a "sponge" that filled with liquid for extraction, in which analytes successfully transferred from the mobile aqueous phase under constant flow rate into organic phase to achieve filtration-based adsorption; similarly, the utilization of fresh organic solvent under a slightly higher flow rate came into contact with the confined solvent and transferred the analytes into the mobile organic phase, thus accomplishing desorption. In order to verify this hypothesis of desorption, the optimal flow rates and desorption volume of organic solvent were sequentially examined. As the ideal type of confined solvent for adsorption, HEX was also selected as the organic solvent for desorption, and the optimization results were indicated in Figure 3. Figure 3(a) showed the optimum flow rate for desorption was 50 mL min^{-1}, which achieved the desorption efficiency of 95.4% with RSD values of less than 5.8%. The desorption efficiencies decreased with the increase in desorption flow rates, which might be attributed to the lack of sufficient contact time for effective mass transfer. As for selecting an ideal desorption solvent volume, at least 100 μL is adequate to desorb 50 μL confined solvent from the material, as displayed in Figure 3(b). It was proven that this non-invasive desorption method greatly maintains the stability and integrity of the composite material, therefore the repeatability of the material can be greatly increased.

3.3 Influence of ethanol content in ginseng extracts

It is essential to explore the influence of ethanol content in ginseng extracts as it was used to extract the intrinsic bioactive ingredients, unfortunately most chlorinated pesticides are also partially soluble in ethanol. Thus, these pesticide residues are co-extracted into the ginseng extract and become an interference that must be removed. Such circumstance signifies the significance of separation method to maintain effectiveness in ginseng extract with ethanol content. In accordance to this demand,

three different ratios of mixed alcohol-water extracts with 15, 25 and 35% ethanol content at different polarities were systematically assessed.[7] Their polarity indices [39–41] were showed in Figure 4(a). It can be seen from Figure 4(a) that the elimination rate of pesticide residues was significantly reduced in the ginseng solution with 35% ethanol content. The maximum anti-alcohol ability of this method is recorded at 25% ethanol content in ginseng extract, with over 80.4% removal rate of pesticide residues and RSDs of less than 12.9%. The anti-alcohol mechanism is probably due to the competitive adsorption of different targets by the solvent. It can be explained by referring to the polarity index, in which the increment of ethanol content is inversely proportionate to the overall polarity of the mixed solution. Compared with the aqueous solution, the retention (adsorption) ability of organic solvent towards pesticide residues was significantly improved. It was proven that changing the type of confined solvent from water to organic solvent can substantially improve the anti-alcohol ability for adsorbing the non-polar pesticides in industrial ethanol-containing ginseng extract. As far as we are concerned, it is also the first study that attempts to remove pesticide residues in ginseng extracts with ethanol content, which provides valuable scientific information for facilitating industrial application.

3.4 Validation of the developed method

The repeatability of the CNFs/CFs material was one of the important parameters for evaluating the performance of the method. Under the optimized desorption conditions for analyzing ginseng extract, the results of desorption rate were no less than 95%, indicating that the CNFs/CFs could be recycled. The adsorption efficiency of the CNFs/CFs towards selected pesticides was still over 82.5% after 10 cycles, as shown in Figure 4(b).

In order to further prove the application of this method for eliminating pesticides in ginseng extract, the number of chlorinated pesticides was increased from four to nineteen. Under optimized condition, the analytical method proposed in this study was validated through evaluating the linearity, accuracy, precision and sensitivity. As shown in Table 2, good linearity with the square of the correlation coefficient (R^2 > 0.99) was obtained for all the analyzed compounds. The intra- and inter-day recoveries were in the range of 85.5 - 97.5% with RSDs < 11.8%, proving the excellent stability and reproducibility of this filtration system. The method limit of detections (MLODs) for selected chlorinated pesticides ranged from 2.22 to 61.55 ng g^{-1}, indicating the satisfactory detection limit and sensitivity of the CNFs-NLPF technique.

The analytical performance of the CNFs-NLPF method for eliminating organic pollutants was compared with similar filtration-based techniques (Table 3), which highlighted the significant advantages of this filtration system, especially from the flow rate and reusability perspectives.

3.5 Analysis of chlorinated pesticides in ginseng samples and future prospects

In order to justify the feasibility of applying this removal method at industrial level, scaled-up filtration experiments were proposed through analyzing larger volume (1 L) of ginseng extract under the optimal parameters. It can be seen from Figure 4(c) that similar results were obtained for removing pesticide residues from large-volume ginseng samples, which achieved 88.3 - 95.4% removal rate of pesticide residues and RSDs of less than 11.8%. Such performance fully demonstrated the feasibility of the CNFs-NLPF method to be further modified as a simple and effective industrial-grade device to remove pesticide residues in ginseng extract.

The applicability of the proposed method was verified through employing it to investigate the occurrence of chlorinated pesticides in different ginseng products

available for purchase in the traditional Chinese medicine store. Results showed that none of the tested chlorinated pesticides were observed in all the ginseng samples.

The CNFs-NLPF technique validated its effectiveness to selectively eliminate nineteen chlorinated pesticides from ginseng extracts, while retaining ginsenosides with minimal losses through confined non-polar solvent that facilitated liquid phase nanoextraction on the CNFs/CFs surface. Most importantly, this method was proved successful in removing pesticide residues in industrial ginseng extract with ethanol content. In addition to the rapid and simple characteristics of the CNFs-NLPF method, the reusability of the material is also a vital strength. This method had proved feasible to be scaled-up or modified for filtering a large volume of ginseng extract, which also achieved excellent removal of pesticide residues within a short period of time. The feasibility for up-scaling this method provides a promising method for removing pesticide residues in the ginseng industry, which aids in offering technical basis that coupled with application prospects to advance the food safety sector.

ASSOCIATED CONTENT

Author Information

*Corresponding author

E-mail: dhli@ybu.edu.cn; Phone: +86-0433-2436456; Fax: +86-0433-2732456

ORCID: 0000-0002-7033-6672

Funding

This study was supported by a grant from the National Natural Science Foundation of China (No. 21775134, 2018C042-3).

Declaration of interest

There are no conflicts of interest to declare.

Abbreviations used

NLPF, nanoconfined liquid phase filtration; CNFs/CFs, carbon nanofibers/carbon fibers; CNFs-NLPF, carbon nanofibers-nanoconfined liquid phase filtration; MBBR, moving bed biofilm reactor; AOPs, advanced oxidation processes; LLE, liquid-liquid extraction; CVD, chemical vapor deposition method; NLPNE, nanoconfined liquid phase nanoextraction; ACE, acetone; DCM, dichloromethane; HEX, hexane; ACN, acetonitrile; MeOH, methanol; EtOH, ethanol; α-HCH, alpha-hexachlorocyclohexane; Lindane, gamma-hexachlorocyclohexane; δ-HCH, delta-hexachlorocyclohexane; PCNB, pentachloronitrobenzene; DDE, dichlorodiphenyldichloroethylene; DDD, dichlorodiphenyldichloroethane; DDT, dichlorodiphenyltrichloroethane; TPP, Triphenyl phosphine; TCM, Traditional Chinese medicine; GC-MS, gas chromatography-mass spectrometry; SIM, selected ion monitoring; LC-MS/MS, liquid chromatography-tandem mass spectrometry; HPLC-ESI-MS/MS, high performance liquid chromatography-electron spray ionization-tandem mass spectrometry; MRM, multiple reaction monitoring; C18, bonded octadecyl silica; PES, polyethersulfone; SEM, scanning electron microscope; RSD, relative standard deviation; MLOD, method limit of detection; LOD, limit of detection.

REFERENCES

(1) Attele, A. S.; Wu, J. A.; Yuan, C.-S. Ginseng Pharmacology. *Biochem. Pharmacol.* **1999**, *58* (11), 1685–1693. https://doi.org/10.1016/S0006-2952(99)00212-9.

(2) Lu, J.-M.; Yao, Q.; Chen, C. Ginseng Compounds: An Update on Their Molecular Mechanisms and Medical Applications. *Curr. Vasc. Pharmacol.* **2009**, *7* (3), 293–302. https://doi.org/10.2174/157016109788340767.

(3) Won, H.-J.; Kim, H. I.; Park, T.; Kim, H.; Jo, K.; Jeon, H.; Ha, S. J.; Hyun, J. M.; Jeong, A.; Kim, J. S.; Park, Y. J.; Eo, Y. H.; Lee, J. Non-Clinical Pharmacokinetic Behavior of Ginsenosides. *J. Ginseng Res.* **2019**, *43* (3), 354–360. https://doi.org/10.1016/j.jgr.2018.06.001.

(4) Kulkarni, J.; Kapse, N.; Kulkarni, D. Plant-Based Pesticide for Control of Helicoverpa Armigera on Cucumis Sativus. *Asian Agri-Hist.* **2009**, *14* (4), 327–332.

(5) Qu, J.; Xu, Y.; Ai, G.-M.; Liu, Y.; Liu, Z.-P. Novel Chryseobacterium Sp. PYR2 Degrades Various Organochlorine Pesticides (OCPs) and Achieves Enhancing Removal and Complete Degradation of DDT in Highly Contaminated Soil. *J. Environ. Manage.* **2015**, *161*, 350–357. https://doi.org/10.1016/j.jenvman.2015.07.025.

(6) Winter, C. K. Pesticide Residues in Imported, Organic, and "Suspect" Fruits and Vegetables. *J. Agric. Food Chem.* **2012**, *60* (18), 4425–4429. https://doi.org/10.1021/jf205131q.

(7) Cha, K.-M.; Lee, E.-S.; Kim, I.-W.; Cho, H.-K.; Ryu, J.-H.; Kim, S.-K. Canola Oil Is an Excellent Vehicle for Eliminating Pesticide Residues in Aqueous Ginseng Extract. *J. Ginseng Res.* **2016**, *40* (3), 292–299. https://doi.org/10.1016/j.jgr.2015.09.007.

(8) Alavanja, M. C. R.; Bonner, M. R. Occupational Pesticide Exposures and Cancer Risk: A Review. *J. Toxicol. Environ. Health Part B* **2012**, *15* (4), 238–263. https://doi.org/10.1080/10937404.2012.632358.

(9) Bachmann Pinto, H.; Miguel de Souza, B.; Dezotti, M. Treatment of a Pesticide Industry Wastewater Mixture in a Moving Bed Biofilm Reactor Followed by Conventional and Membrane Processes for Water Reuse. *J. Clean. Prod.* **2018**, *201*, 1061–1070. https://doi.org/10.1016/j.jclepro.2018.08.113.

(10) Torresi, E.; Fowler, S. J.; Polesel, F.; Bester, K.; Andersen, H. R.; Smets, B. F.; Plósz, B. Gy.; Christensson, M. Biofilm Thickness Influences Biodiversity in Nitrifying MBBRs—Implications on Micropollutant Removal. *Environ. Sci. Technol.* **2016**, *50* (17), 9279–9288. https://doi.org/10.1021/acs.est.6b02007.

(11) Gar Alalm, M.; Tawfik, A.; Ookawara, S. Comparison of Solar TiO 2 Photocatalysis and Solar Photo-Fenton for Treatment of Pesticides Industry Wastewater: Operational Conditions, Kinetics, and Costs. *J. Water Process Eng.* **2015**, *8*, 55–63. https://doi.org/10.1016/j.jwpe.2015.09.007.

(12) Chuang, Y.-H.; Chen, S.; Chinn, C. J.; Mitch, W. A. Comparing the UV/Monochloramine and UV/Free Chlorine Advanced Oxidation Processes (AOPs) to the UV/Hydrogen Peroxide AOP Under Scenarios Relevant to Potable Reuse. *Environ. Sci. Technol.* **2017**, *51* (23), 13859–13868. https://doi.org/10.1021/acs.est.7b03570.

(13) Li, G.; Sun, L.; Tang, S. Combination of Supercritical Fluid Elution and Resin Adsorption for Removal of Procymidone from Ginseng Extracts. *Korean J. Chem. Eng.* **2018**, *35* (4), 956–963. https://doi.org/10.1007/s11814-018-0001-4.

(14) Yao, L.; Zhang, N.; Wang, C.; Wang, C. Highly Selective Separation and Purification of Anthocyanins from Bilberry Based on a Macroporous Polymeric Adsorbent. *J. Agric. Food Chem.* **2015**, *63* (13), 3543–3550. https://doi.org/10.1021/jf506107m.

(15) Handlos, A. E.; Baron, T. Mass and Heat Transfer from Drops in Liquid-Liquid Extraction. *AIChE J.* **1957**, *3* (1), 127–136. https://doi.org/10.1002/aic.690030121.

(16) Zhang, Y.; Lee, H. K. Liquid Phase Microextraction Using Knitting Wool as the Extractant Phase Holder before Chromatographic Analysis: A New Approach for Trace Analysis. *J. Chromatogr. A* **2013**, *1273*, 12–17. https://doi.org/10.1016/j.chroma.2012.11.084.

(17) Nurerk, P.; Liew, C. S. M.; Bunkoed, O.; Kanatharana, P.; Lee, H. K. Environmentally Friendly Etching of Stainless Steel Wire for Plunger-in-Needle Liquid-Phase Microextraction of Polycyclic Aromatic Hydrocarbons. *Talanta* **2019**, *197*, 465–471. https://doi.org/10.1016/j.talanta.2019.01.046.

(18) Li, Q.; Sun, X.; Li, Y.; Xu, L. Hydrophobic Melamine Foam as the Solvent Holder for Liquid–Liquid Microextraction. *Talanta* **2019**, *191*, 469–478. https://doi.org/10.1016/j.talanta.2018.09.003.

(19) Bradford, P. D.; Wang, X.; Zhao, H.; Zhu, Y. T. Tuning the Compressive Mechanical Properties of Carbon Nanotube Foam. *Carbon* **2011**, *49* (8), 2834–2841. https://doi.org/10.1016/j.carbon.2011.03.012.

(20) Maensiri, S.; Laokul, P.; Klinkaewnarong, J.; Amornkitbamrung, V. Carbon Nanofiber-Reinforced Alumina Nanocomposites: Fabrication and Mechanical Properties. *Mater. Sci. Eng. A* **2007**, *447* (1–2), 44–50. https://doi.org/10.1016/j.msea.2006.08.009.

(21) Meng, L.-Y.; Moon, C.-W.; Im, S.-S.; Lee, K.-H.; Byun, J.-H.; Park, S.-J. Effect of Ni Catalyst Dispersion on the Growth of Carbon Nanofibers onto Carbon Fibers. *Microporous Mesoporous Mater.* **2011**, *142* (1), 26–31. https://doi.org/10.1016/j.micromeso.2010.10.008.

(22) Zou, Y.; Wang, L.; Sun, H.; Wang, G.; Meng, L.-Y.; Quinto, M.; Li, D. Nanoconfined Liquid Phase Nanoextraction Based on Carbon Nanofibers. *Anal. Chem.* **2021**, *93* (3), 1310–1316. https://doi.org/10.1021/acs.analchem.0c01462.

(23) Kim, S.-A.; Jeong, E.-B.; Oh, D.-K. Complete Bioconversion of Protopanaxadiol-Type Ginsenosides to Compound K by Extracellular Enzymes from the Isolated Strain *Aspergillus Tubingensis*. *J. Agric. Food Chem.* **2021**, *69* (1), 315–324. https://doi.org/10.1021/acs.jafc.0c07424.

(24) Park, S.-E.; Na, C.-S.; Yoo, S.-A.; Seo, S.-H.; Son, H.-S. Biotransformation of Major Ginsenosides in Ginsenoside Model Culture by Lactic Acid Bacteria. *J. Ginseng Res.* **2017**, *41* (1), 36–42. https://doi.org/10.1016/j.jgr.2015.12.008.

(25) Dong, W.-W.; Xuan, F.-L.; Zhong, F.-L.; Jiang, J.; Wu, S.; Li, D.; Quan, L.-H. Comparative Analysis of the Rats' Gut Microbiota Composition in Animals with Different Ginsenosides Metabolizing Activity. *J. Agric. Food Chem.* **2017**, *65* (2), 327–337. https://doi.org/10.1021/acs.jafc.6b04848.

(26) Zhang, L.; Shen, H.; Xu, J.; Xu, J.-D.; Li, Z.-L.; Wu, J.; Zou, Y.-T.; Liu, L.-F.; Li, S.-L. UPLC-QTOF-MS/MS-Guided Isolation and Purification of Sulfur-Containing Derivatives from Sulfur-Fumigated

505 Edible Herbs, a Case Study on Ginseng. *Food Chem.* **2018**, *246*, 202–210.
506 https://doi.org/10.1016/j.foodchem.2017.10.151.

507 (27) Park, S.-J.; Shin, J.-S.; Shim, J.-W.; Ryu, S.-K. Effect of Acidic Treatment on Metal Adsorptions
508 of Pitch-Based Activated Carbon Fibers. *J. Colloid Interface Sci.* **2004**, *275* (1), 342–344.
509 https://doi.org/10.1016/j.jcis.2004.01.010.

510 (28) Zheng, F.; Liang; Gao, Y.; Sukamto, J. H.; Aardahl, C. L. Carbon Nanotube Synthesis Using
511 Mesoporous Silica Templates. *Nano Lett.* **2002**, *2* (7), 729–732. https://doi.org/10.1021/nl025558e.

512 (29) Chen, L.; Yin, L.; Song, F.; Liu, Z.; Zheng, Z.; Xing, J.; Liu, S. Determination of Pesticide
513 Residues in Ginseng by Dispersive Liquid–Liquid Microextraction and Ultra High Performance Liquid
514 Chromatography–Tandem Mass Spectrometry. *J. Chromatogr. B* **2013**, *917–918*, 71–77.
515 https://doi.org/10.1016/j.jchromb.2012.12.034.

516 (30) Kaw, H. Y.; Li, J.; Jin, X.; Wang, Z.; Cong, L.; He, M.; Li, D. Ultrasound-Assisted Liquid–Liquid
517 Spray Extraction for the Determination of Multi-Class Trace Organic Compounds in High-Volume
518 Water Samples. *The Analyst* **2018**, *143* (19), 4575–4584. https://doi.org/10.1039/C8AN00656C.

519 (31) Beveridge, T. H. J.; Li, T. S. C.; Drover, J. C. G. Phytosterol Content in American Ginseng Seed
520 Oil. *J. Agric. Food Chem.* **2002**, *50* (4), 744–750. https://doi.org/10.1021/jf010701v.

521 (32) Jung, C.-H.; Seog, H.-M.; Choi, I.-W.; Cho, H.-Y. Antioxidant Activities of Cultivated and Wild
522 Korean Ginseng Leaves. *Food Chem.* **2005**, *92* (3), 535–540.
523 https://doi.org/10.1016/j.foodchem.2004.08.021.

524 (33) Lee, S. D.; Yoo, G.; Chae, H. J.; In, M.-J.; Oh, N.-S.; Hwang, Y. K.; Hwang, W. I.; Kim, D. C.
525 Lipid-Soluble Extracts as the Main Source of Anticancer Activity in Ginseng and Ginseng Marc. *J. Am.*
526 *Oil Chem. Soc.* **2009**, *86* (11), 1065–1071. https://doi.org/10.1007/s11746-009-1460-x.

527 (34) Gulluce, M.; Agar, G.; Baris, O.; Karadayi, M.; Orhan, F.; Sahin, F. Mutagenic and
528 Antimutagenic Effects of Hexane Extract of Some *Astragalus* Species Grown in the Eastern Anatolia
529 Region of Turkey: MUTAGENIC AND ANTIMUTAGENIC EFFECTS OF SOME *ASTRAGALUS SPECIES*.
530 *Phytother. Res.* **2010**, *24* (7), 1014–1018. https://doi.org/10.1002/ptr.3059.

531 (35) Buffa, A.; Mandler, D. Adsorption and Detection of Organic Pollutants by Fixed Bed Carbon
532 Nanotube Electrochemical Membrane. *Chem. Eng. J.* **2019**, *359*, 130–137.
533 https://doi.org/10.1016/j.cej.2018.11.069.

534 (36) Li, L.; Zhang, J.; Li, Y.; Yang, C. Removal of Cr (VI) with a Spiral Wound Chitosan Nanofiber
535 Membrane Module via Dead-End Filtration. *J. Membr. Sci.* **2017**, *544*, 333–341.
536 https://doi.org/10.1016/j.memsci.2017.09.045.

537 (37) Cao, A. Super-Compressible Foamlike Carbon Nanotube Films. *Science* **2005**, *310* (5752),
538 1307–1310. https://doi.org/10.1126/science.1118957.

539 (38) Falvo, M. R.; Clary, G. J.; Taylor, R. M.; Chi, V.; Brooks, F. P.; Washburn, S.; Superfine, R.
540 Bending and Buckling of Carbon Nanotubes under Large Strain. *Nature* **1997**, *389* (6651), 582–584.
541 https://doi.org/10.1038/39282.

542 (39) Snyder, L. R. Classification off the Solvent Properties of Common Liquids. *J. Chromatogr. Sci.*
543 **1978**, *16* (6), 223–234. https://doi.org/10.1093/chromsci/16.6.223.

(40) Zhang, Q.; Liu, R.; Xu, H.; Yang, X.; Zhang, Y.; Wang, Q.; Gao, P.; Bi, K.; Han, T.; Li, Q. Multifunctional Isotopic Standards Based Steroidomics Strategy: Exploration of Cancer Screening Model. *J. Chromatogr. A* **2020**, *1614*, 460723. https://doi.org/10.1016/j.chroma.2019.460723.

(41) Yu, C.; Zhang, Q.; Zou, Y.; Liu, R.; Zhao, J.; Bi, K.; Li, D.; Li, Q. Across-Polarity Quantification Method for Broad Metabolome Coverage Based on Consecutive Nanoconfined Liquid Phase Nanoextraction Technology: Application in Discovering the Plasma Potential Biomarkers of Different Types of Cancer. *Anal. Chim. Acta* **2021**, *1167*, 338577. https://doi.org/10.1016/j.aca.2021.338577.

(42) Zhu, Y.; Wei, J.; Zhang, H.; Liu, K.; Kong, Z.; Dong, Y.; Jin, G.; Tian, J.; Qin, Z. Fabrication of Composite Membrane with Adsorption Property and Its Application to the Removal of Endocrine Disrupting Compounds during Filtration Process. *Chem. Eng. J.* **2018**, *352*, 53–63. https://doi.org/10.1016/j.cej.2018.06.182.

(43) Lam, B.; Déon, S.; Morin-Crini, N.; Crini, G.; Fievet, P. Polymer-Enhanced Ultrafiltration for Heavy Metal Removal: Influence of Chitosan and Carboxymethyl Cellulose on Filtration Performances. *J. Clean. Prod.* **2018**, *171*, 927–933. https://doi.org/10.1016/j.jclepro.2017.10.090.

(44) Chakraborty, S.; O'Malley, R. J.; Bartlett, L.; Xu, M. Removal of Alumina Inclusions from Molten Steel by Ceramic Foam Filtration. *Int. J. Met.* **2020**. https://doi.org/10.1007/s40962-020-00537-9.

Figure Captions:

Figure 1 SEM images of the surface of (a) bare CF and (b) CNFs/CF.

Figure 2 Influential factors that affect the separation performance of CNFs-NLPF, including (a) types of confined solvent, (b) breakthrough curves and (c) filtration rate. *Asterisk* signifies the statistically significant difference ($p < 0.01$ **, $p < 0.001$ ***).

Figure 3 Influential factors that affect the desorption efficiency of CNFs-NLPF, including (a) desorption rate and (b) desorption solvent volume. *Asterisk* signifies the statistically significant difference ($p < 0.05$ *, $p < 0.01$ **, $p < 0.001$ ***).

Figure 4 (a) Effects of ethanol content on the separation efficiency of pesticides and ginsenosides, (b) Adsorption efficiency of selected pesticides by reused CNFs/CFs after ten filtration cycles, (c) Comparison of removal rate for pesticide residues by using small-scale and scale-up versions of the CNFs-NLPF.

591 Table 1: Retention time, quantification ion and qualitative ions of nineteen chlorinated
592 pesticides analyzed by GC-MS, and MRM parameters for seven ginsenosides analyzed
593 by LC-MS/MS.

GC-MS	Pesticides	Retention time (min)	Quantitative ion	Qualitative ion 1	Qualitative ion 2
1	α-HCH	9.14	219	183	181
2	PCNB	9.99	295	237	249
3	Lindane	10.19	219	183	181
4	δ-HCH	11.18	219	183	181
5	Heptachlor	12.57	272	274	270
6	Aldrin	13.80	263	265	293
7	Heptachlor epoxide	15.19	353	355	351
8	Procymidone	15.64	283	285	255
9	Endosulfan-A	16.50	241	277	339
10	DDE	17.38	318	316	246
11	Dieldrin	17.48	263	277	380
12	Endrin	18.22	263	317	345
13	Endosulfan-B	18.65	241	277	339
14	DDD	18.92	235	237	165
15	Endrin aldehyde	19.18	345	250	281
16	Endosulfan sulfate	20.05	272	274	229
17	DDT	20.27	235	237	165
18	Endrin ketone	21.72	317	250	319
19	Methoxychlor	22.34	227	228	212
LC-MS/MS	Ginsenosides	Precursor Ion	Product Ion	Fragment (V)	Collision Energy
1	Rb1	1131.3	789.3	250	60
2	Rb2	1101.7	789.6	250	60
3	Rc	1101.7	789.6	250	60
4	Re	969.5	789.2	135	50
5	Rd	969.5	789.2	135	50
6	Rg1	823.4	643.6	250	40
7	Rf	823.3	365.0	250	60

594

595

596

597 Table 2: Analytical performance of the CNFs-NLPF method based on square of
598 correlation coefficient (R^2), intra- and inter-day recoveries, relative standard deviation
599 (RSD), detection limit (LOD) and method limit of detection (MLOD).

	R^2	Intra-day recovery (%)	RSD (n = 3)	Inter-day recovery (%)	RSD (n = 3)	LOD (ng g^{-1})	MLOD (ng g^{-1})
α-HCH	0.9997	85.9	2.6	90.6	11.3	3.88	7.66
PCNB	0.9992	86.7	3.9	93.4	3.5	3.32	11.90
Lindane	0.9991	94.6	2.7	91.4	4.2	5.87	8.08
δ-HCH	0.9993	94.7	1.4	87.6	2.2	8.42	13.73
Heptachlor	0.9992	88.5	8.2	90.6	5.8	1.37	2.28
Aldrin	0.9993	92.6	7.6	96.4	11.1	1.74	2.22
Heptachlor epoxide	0.9988	90.3	2.7	91.4	8.9	8.57	9.96
Procymidone	0.9994	85.5	3.6	87.6	7.4	1.80	5.32
Endosulfan-A	0.9991	88.5	4.7	90.6	11.8	18.02	30.93
DDE	0.9989	88.1	8.6	96.4	5.6	3.84	5.33
Dieldrin	0.9989	97.5	4.7	91.4	8.2	7.09	15.85
Endrin	0.9992	94.1	7.3	87.6	6.6	28.44	37.27
Endosulfan-B	0.9992	88.5	8.5	90.6	9.5	18.13	32.73
DDD	0.9997	93.8	4.3	96.4	6.8	8.42	11.90
Endrin aldehyde	0.9993	90.7	4.1	91.4	8.2	25.00	41.95
Endosulfan sulfate	0.9993	94.6	2.7	87.6	3.9	14.53	24.81
DDT	0.9995	90.5	3.5	90.6	8.5	6.05	5.88
Endrin ketone	0.9994	85.7	2.9	96.4	7.3	27.52	61.55
Methoxychlor	0.9995	89.3	5.3	91.4	8.6	3.99	5.97

600
601
602
603
604
605
606

607 Table 3: Comparison of the performances between different adsorbents in the filtration-

608 based systems for pollutant removal.

609

Adsorbent	Flow rate	Reusability	References
CNFs/CFs	45 mL min^{-1}	10	this study
Spiral wound chitosan nanofiber	15 mL min^{-1}	3	[36]
PP-g-SA HEA	10 mL min^{-1}	5	[42]
Polyamide composite flat-sheet membrane	4 m s^{-1}	-	[43]
Ceramic foam	0.45 m s^{-1}	-	[44]

610 PP-g-SA HEA: polypropylene-grafting-stearyl acrylate hydroxyethyl acrylate

611

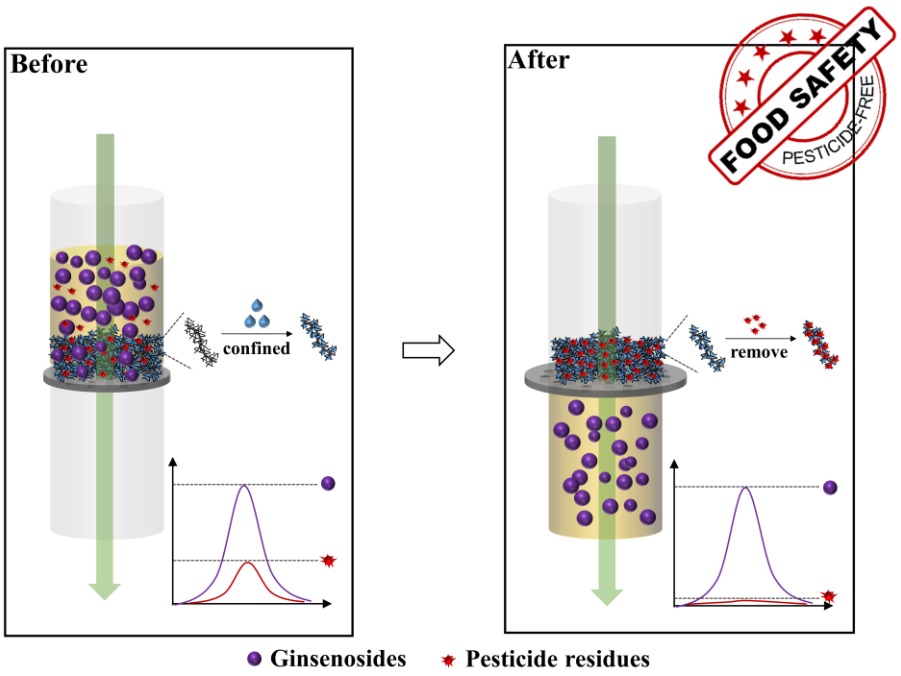

612

613 Graphical abstract

614

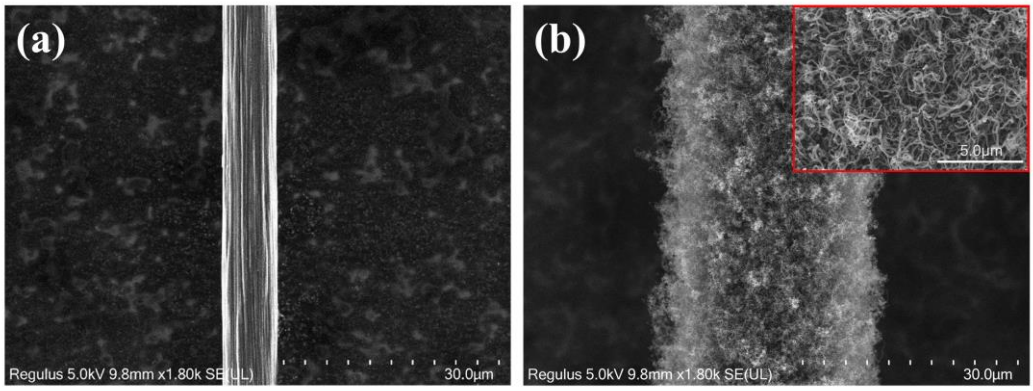

615

616 Figure 1

617

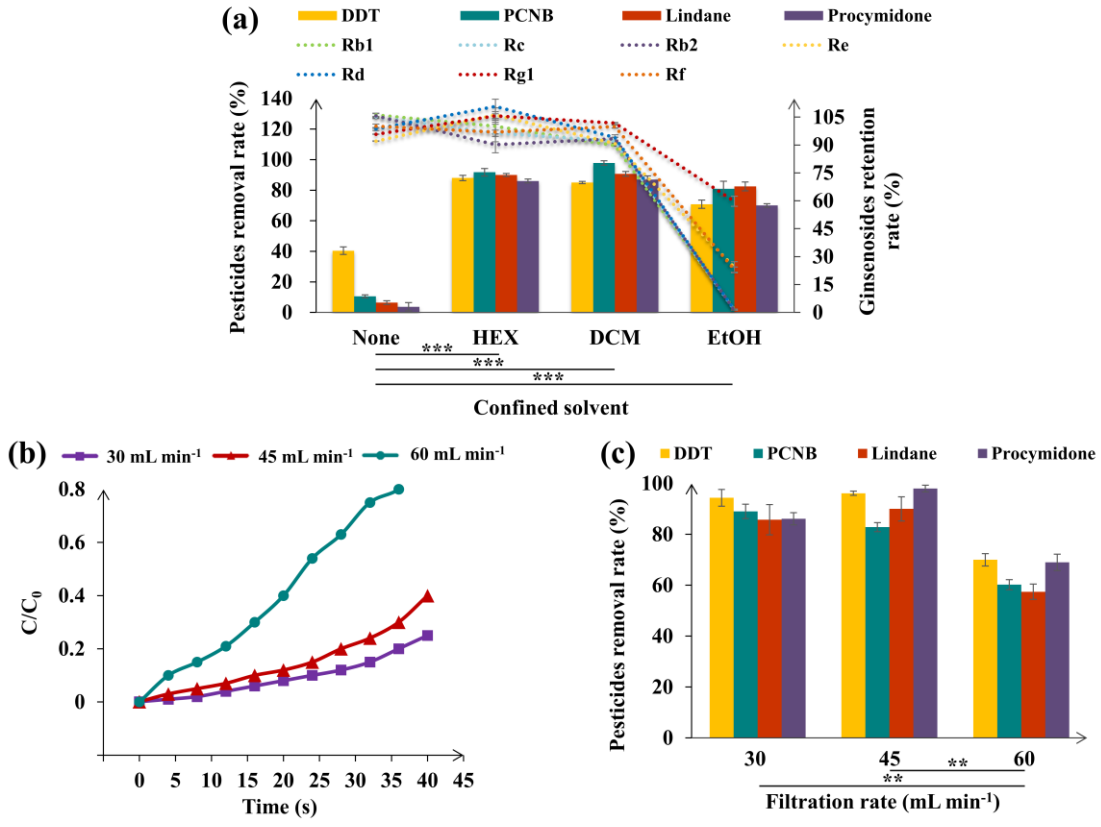

618

619 Figure 2

620

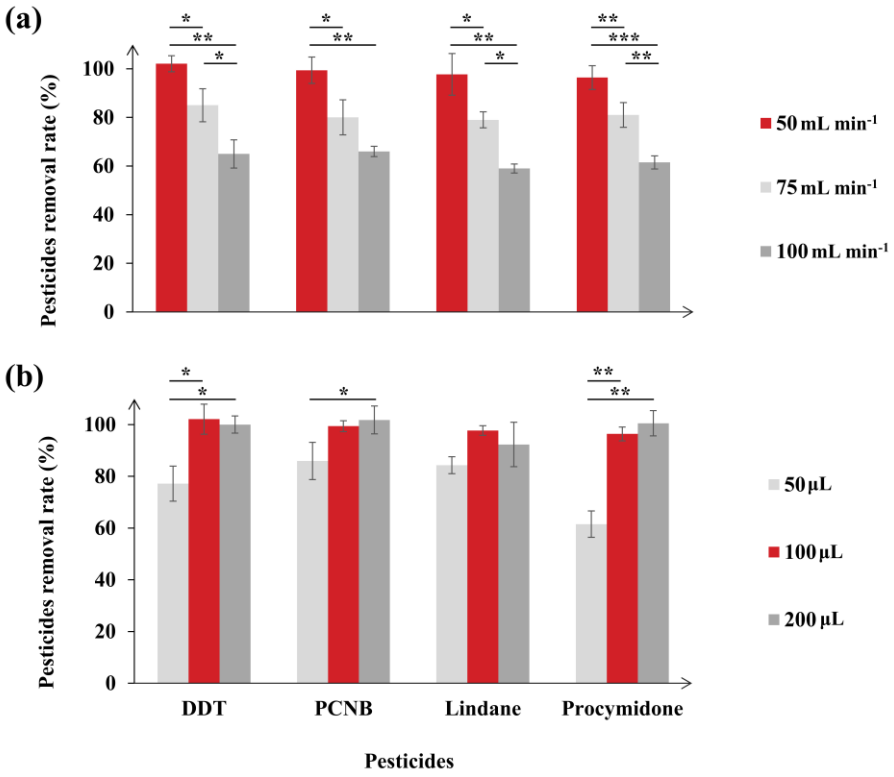

621

622

623 Figure 3

624

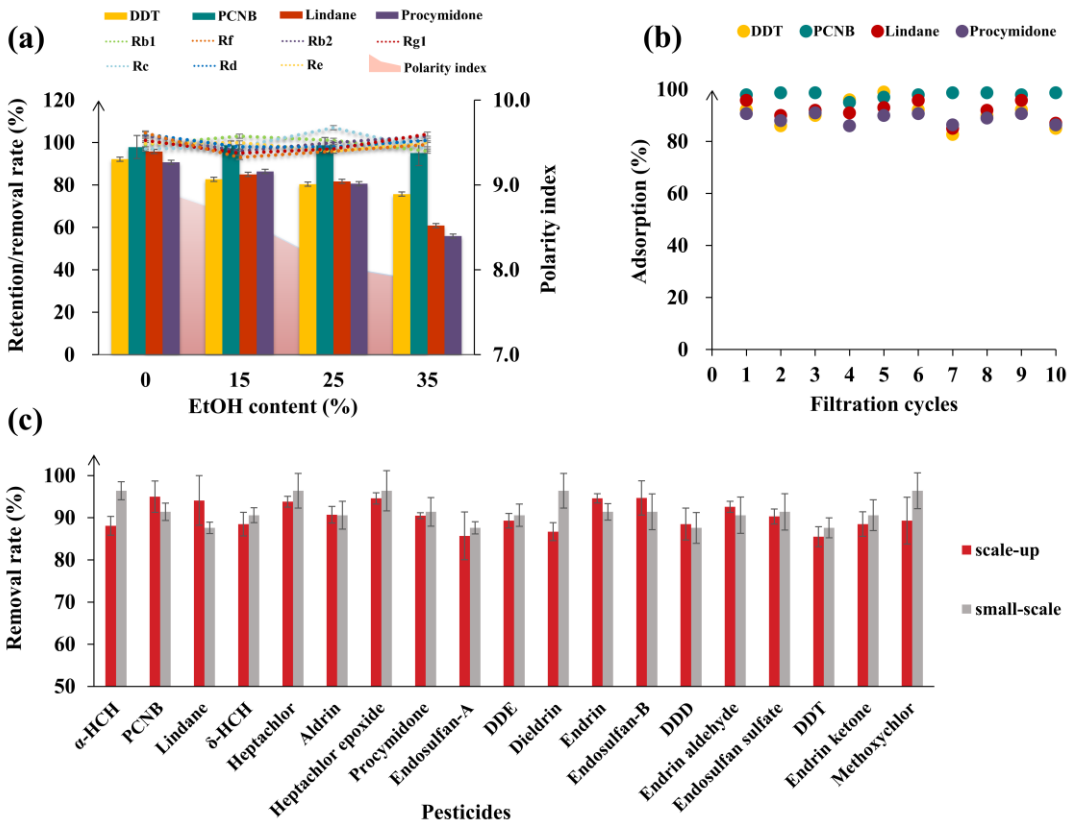

625

626 Figure 4